RSC Advances

PAPER

View Article Online
View Journal | View Issue

Cite this: *RSC Adv.*, 2016, **6**, 5491

Base free synthesis of iron oxide supported on boron nitride for the construction of highly functionalized pyrans and spirooxindoles†

Aniruddha Molla and Sahid Hussain*

Received 20th October 2015
Accepted 31st December 2015

DOI: 10.1039/c5ra21969h

www.rsc.org/advances

Boron nitride supported iron oxide (BN@Fe_3O_4) network was achieved *via* chemical reduction followed by aerial oxidation in absence of base. The prepared BN@Fe_3O_4 was characterized by powder XRD, FT-IR, Raman, BET and FE-SEM. The catalytic property was subsequently investigated for one-pot multicomponent domino reaction for the synthesis of highly functionalized pyrans and spirooxindoles derivatives on water. The present method is simple, high yielding, recyclable and requires no column chromatography.

Introduction

Heterogeneous catalysis has been known for many years and become expediently essential for efficient organic transformations over the past few years.[1,2] 'Nanocatalysis' is an important growing field in catalysis science because of its small size and high surface area and thereby reducing the amount of catalyst and cost.[3,4] Due to the difficulties in separation of nanocatalyst, chemists started to use solid-supports to make it heterogeneous. Solid-supported catalysts are vital and mounting field in semi-heterogeneous catalysis[5] where surface functionalization of non-magnetic nanoparticles with ligands provides a well-designed way to bridge the gap between heterogeneous and homogeneous catalysis.[6]

Boron nitride (BN), consists of equal numbers of boron and nitrogen atoms, is isoelectronic with carbon in cubic and hexagonal forms and is analogous to graphite. The strong B–N covalent bonds within hexagonal boron nitride (h-BN) impart high mechanical, thermal and chemical stability. In view of the above, BN has earned notice in the field of heterogeneous catalysis over the past decade.[7–9] One of the important interesting features of BN is that it behaves as both Lewis acid and Lewis base.[10] To enhance ease of separation and Lewis basicity, we thought to incorporate iron oxide on BN. In the last few years, different forms of iron oxides [such as FeO (wustite), Fe_2O_3 (iron III oxides), α-Fe_2O_3 (hematite), β-Fe_2O_3 (beta phase), and γ-Fe_2O_3 (maghemite)] were extensively used as a powerful catalyst for many organic transformations due to its special features like less toxic, stable, inexpensive, and recyclable.[11–15] A wide variety of methods have been reported in the literature for the synthesis of Fe_3O_4 nanoparticles such as hydrothermal process,[16] sonochemical method,[17] microemulsion technique,[18] electrochemical route,[19] co-precipitation[20] and microwave method.[21–23] In order to synthesize iron oxide on BN, we follow a new technique which involves reduction of Fe^{2+} to Fe^0 followed by aerial oxidation to Fe_3O_4 and then applied to multicomponent reactions.

Multicomponent reactions (MCRs) of more than two substrates offer the maximum potential for molecular diversity in one step and atom economic way, with lowest synthetic time and effort.[24,25] Knoevenagel condensation in combination with Michael addition has been dynamically used for synthesis of highly functionalized pyrans and spirooxindoles derivatives in domino fashion due to its wide medicinal and pharmaceutical application such as anticancer,[26] anti-HIV,[27] antimalarial,[28] antitubercular[29] *etc.* Fig. 1 represents some bioactive pyran derivatives.[30–32] In continuation of our ongoing research on the synthesis of highly functionalized pyran and spirooxindole derivatives[33,34] in domino fashion, we used boron nitride supported iron oxide, BN@Fe_3O_4 as an effective, reusable and proficient catalyst for the transformations.

Materials and methods

Ferrous sulphate heptahydrate [$FeSO_4 \cdot 7H_2O$], hexagonal boron nitride [h-BN] with particle size $\sim$ 1 μm, sodium borohydride [$NaBH_4$], citric acid, and ethanol (EtOH) were all analytical

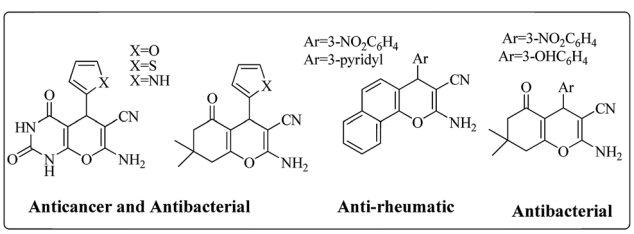

Fig. 1 Pharmacologically active synthetic 2-amino-3-cyano-4*H*-pyran derivatives.

Department of Chemistry, Indian Institute of Technology Patna, Patna 800 013, India. E-mail: sahid@iitp.ac.in; Fax: +91-612-227-7383; Tel: +91-612-255-2022

† Electronic supplementary information (ESI) available: Spectral data of all compounds are available. See DOI: 10.1039/c5ra21969h

grade and used without further purifications. Double distilled water was employed throughout the experiments.

Preparation of BN@Fe_3O_4

BN@Fe_3O_4 was prepared through simple one-pot synthetic method, using citric acid as stabilizing agent. In typical experiment, 100 ml water was added in round bottom flask containing ferrous sulphate hepta-hydrate [$FeSO_4 \cdot 7H_2O$] (2500 mg, 9 mmol), boron nitride (2000 mg, 81 mmol) and citric acid (165 mg, 0.75 mmol) and mixture was vigorously stirred for 10 min. Then sodium borohydride [$NaBH_4$] (600 mg, 15 mmol) was added in slots to the stirring solution and was continued for 10 min. The reaction mixture was allowed to settle down and then was filtered and washed with ethanol and water for at least three times. The residue was kept overnight in open air and was finally collected after dried under vacuum. The formation BN@Fe_3O_4 is pictorially represented in Scheme 1. Fe_3O_4 NPs was prepared by hydrothermal synthesis as reported earlier.[20]

Characterizations methods of catalyst

Fourier transform infrared (FT-IR) spectra were recorded in KBr on a Shimadzu IR Affinity I. Powder X-ray diffraction (PXRD) study was carried out on a Rigaku X-ray diffractometer at a voltage of 35 kV using Cu Kα radiations ($\lambda = 0.15418$ nm) at scanning rate of 1.00° per minute in the 2θ range 10–80°. Raman spectra were recorded using 415 nm laser. Field emission scanning electron microscope (FE-SEM) images were obtained from a Hitachi S-4800 microscope at an operating voltage of 10 kV. The sample was coated with platinum for efficient imaging before being charged.

General procedure for multicomponent reaction using BN@Fe_3O_4

To malononitrile (1.1 mmol) dissolved in water (3 ml) was added an aldehyde/isatin (1.0 mmol) followed by BN@Fe_3O_4 (15 mg) and active methylenic diketo compound (1.0 mmol) (dimedone or 4-hydroxy coumarin or cycloalkan-1,3-dione or ethyl acetoacetate/methyl acetoacetate). The reaction mixture was stirred at 80 °C. The progress of the reaction was monitored by TLC and after completion of the reaction the solid precipitate was filtered off and dissolved it again in ethyl acetate. Catalyst was separated with filtration. Product was collected under reduce pressure using ethyl acetate or CH_2Cl_2. All the products were characterised using NMR, IR and melting point analysis ESI.†

Result and discussion

Catalyst characterization

As described in the experimental section, iron oxide was synthesized on BN support by *in situ* reduction followed by

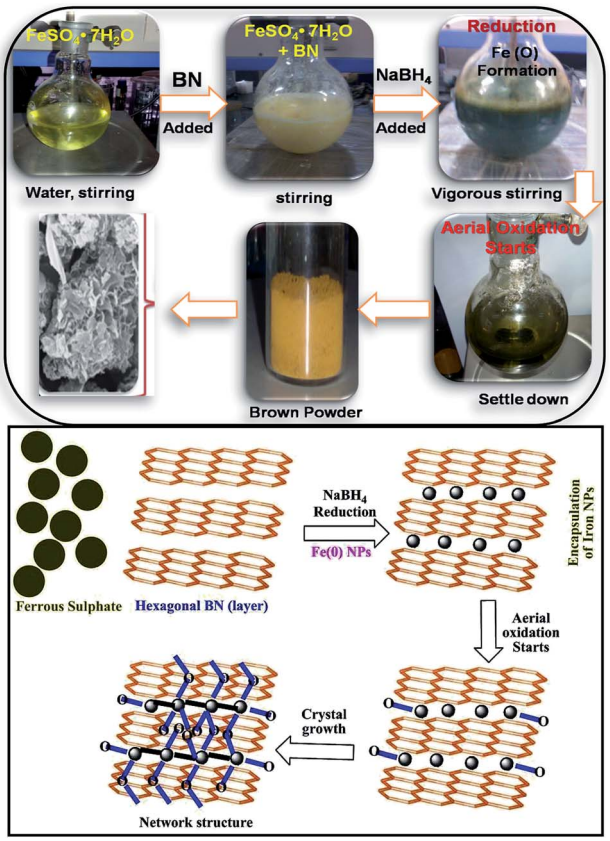

Scheme 1 Proposed strategy for the formation of BN@Fe_3O_4.

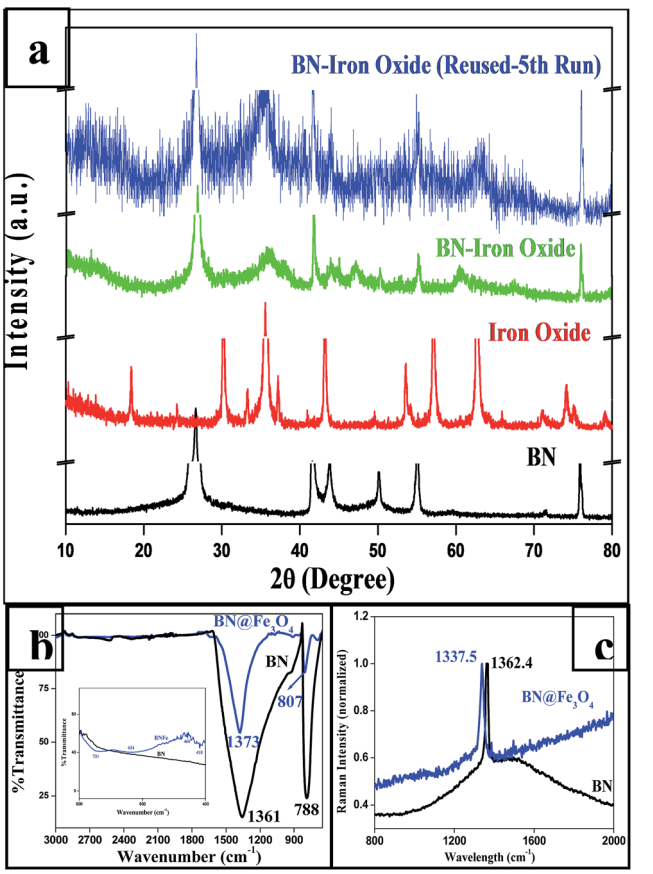

Fig. 2 (a) PXRD of BN, BN@Fe_3O_4 and Fe_3O_4 and BN@Fe_3O_4 reused (after 5th cycle); (b) IR spectra of BN and BN@Fe_3O_4; (c) Raman spectra of BN and BN@Fe_3O_4.

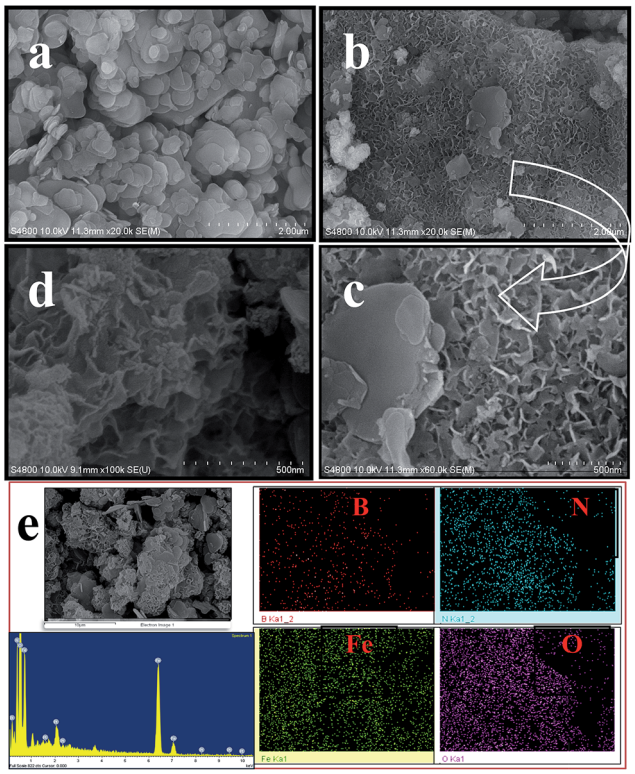

Fig. 3 FE-SEM image of BN (a), BN@Fe_3O_4 (b and c), reused BN@Fe_3O_4 (d) at different magnification, EDX line spectra and elemental mapping of BN@Fe_3O_4 (e).

aerial oxidation. PXRD patterns of BN and BN-supported iron oxide are shown in Fig. 2a. The diffraction peaks (2θ) of hexagonal BN are 26.65° (002), 41.53° (100), 43.84° (101), 50.13° (102), 54.95° (004) and 75.89° (110). After the formation iron oxide on BN, additional peaks were observed at 35.95 and 43.93 that confirm the formation of iron oxide. This was also confirmed with the data taken for iron oxide nanoparticles. The reused catalyst also show similar PXRD patterns with the fresh one substantiating that the catalyst does not change after fifth cycles of it use.

Table 1 Optimization of reaction conditions for **1a**[a]

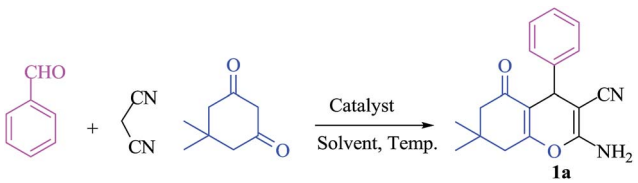

1a

Run	Catalyst (mol%)	Solvent	Temp.	Time (min)	Yield[b] (%)
01	—	H_2O	R.T	180	Trace
02	BN@Fe_3O_4 (01 mg)	H_2O	R.T	180	15
03	BN@Fe_3O_4 (05 mg)	H_2O	R.T	120	25
04	BN@Fe_3O_4 (10 mg)	H_2O	R.T	120	35
05	BN@Fe_3O_4 (10 mg)	EtOH	R.T	120	40
06	BN@Fe_3O_4 (15 mg)	H_2O	R.T	120	60
07	BN@Fe_3O_4 (15 mg)	H_2O	60 °C	60	80
08	**BN@Fe_3O_4 (15 mg)**	**H_2O**	**80 °C**	**10**	**97**
09	BN@Fe_3O_4 (15 mg)	EtOH	Reflux	10	94
10	BN (15 mg)	H_2O	R.T	120	52
11	BN (15 mg)	H_2O	80 °C	30	68
12	Fe_3O_4 (15 mg)	H_2O	80 °C	30	65
13	BN@Fe_3O_4 (20 mg)	H_2O	80 °C	10	97

[a] Reaction conditions: benzaldehyde (1.0 mmol), malononitrile (1.1 mmol) and dimedone (1.0 mmol) in 3 ml solvent. [b] Isolated yield.

Fig. 2b shows the FT-IR spectra of BN and BN@Fe_3O_4. In the spectrum of BN, strong and board peaks at 1361 and 788 cm^{-1} were observed due to B–N stretching and B–N–B bending vibration respectively. The spectrum of BN@Fe_3O_4 shows additional at 731, 634, 460 and 418 which are attributed to Fe–O–Fe and Fe–O bond vibrations.[35] The Raman spectra of the same are presented in Fig. 2c. The unique signal at 1362.4 cm^{-1} is the characteristic of E_{2g} mode of hexagonal-boron nitride. Peak value shift was observed for both IR (B–N stretching, B–N–B bending vibration) and Raman (signature peak for E_{2g} mode) in BN@Fe_3O_4 which might be due to the non-covalent interaction between boron and oxygen.[36,37]

The nitrogen adsorption–desorption isotherm was measured using Smart Instrument, Model No-Smart Prob 92/93 to determine the surface area of the BN@Fe_3O_4. Experiment was performed using N_2 (30%) and He (70%) mixture after the regeneration of the sample. The result shows that, BN have surface area 17.04 $m^2\ g^{-1}$ whereas BN@Fe_3O_4 have surface area 128.62 $m^2\ g^{-1}$. The increase in surface area might be due to the formation of network like structure as observed in FE-SEM image.

The morphologies of BN and BN@Fe_3O_4 were studied by FE-SEM. The FE-SEM image of the samples were taken at different magnification are shown in Fig. 3. Spherical platelets like structure were observed for BN (Fig. 3a) whereas BN@Fe_3O_4 showed network like structures (Fig. 3b–c). The formation of network structure is proposed in Scheme 1. It is believed that network structure forms as a result of two-stage growth process, which involves a fast nucleation of amorphous primary particles followed by a slow aggregation and crystallization of primary particles. In our experiment, Fe(0) is the primary particles that undergo secondary growth with the formation of network structure. Several factors, including crystal-face attraction, electrostatic and dipolar fields associated with the aggregate, hydrophilic interactions, hydrogen bonds and van der Waals forces may have effects on the self-assembly to form final structure.[2,10,12,17,18] The reused catalyst has similar morphology as the fresh one indicating that there is relatively no change in structure after fifth cycles of it use (Fig. 3d).

The composition of BN@Fe_3O_4 was confirmed from Energy-Dispersive X-ray spectroscopy (EDX) analysis and the line spectrum is shown in Fig. 3e. To further study the spatial homogeny of the elemental distribution of BN@Fe_3O_4, EDX elemental mapping was taken. It indicates the homogeneous distribution of B, N, Fe and O elements throughout the sample.

Optimization of catalyst loading

For this study, we optimized reaction condition taking benzaldehyde (1.0 mmol), malononitrile (1.1 mmol) and dimedone (1.0 mmol) as model substrate. The domino effect of catalyst,

Table 2 $BN@Fe_3O_4$ catalyzed synthesis of pyran derivatives with aldehydes, malononitrile and cycloalkane-1,3-dione (**1a–i**)[a] or 1,3-diketoesters (**2a–f**)[a] or 4-hydroxycoumarine (**3a–e**)[a]

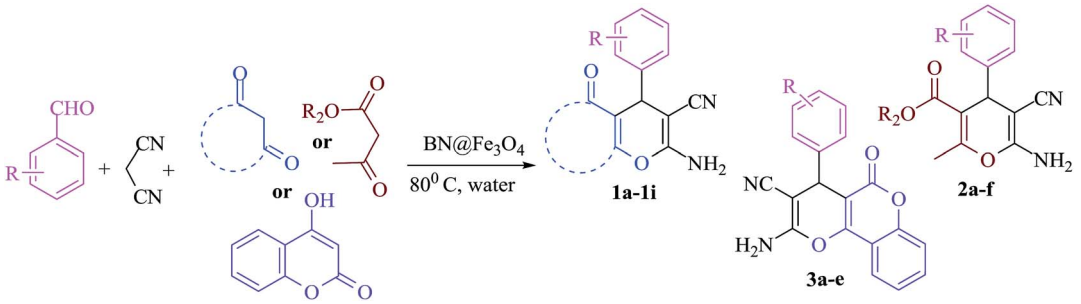

Run	Aldehyde	Diketones/4-hydroxy coumarine	Product	Time (min)	Yield[b] (%)
01	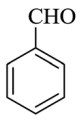	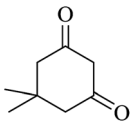	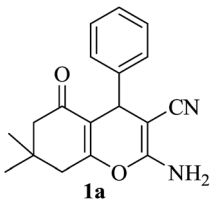 **1a**	10	97 92[c]
02	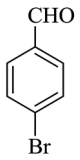	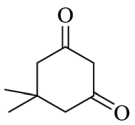	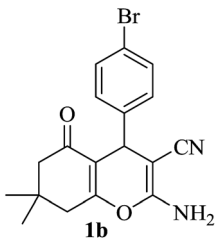 **1b**	10	95
03	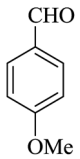	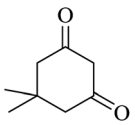	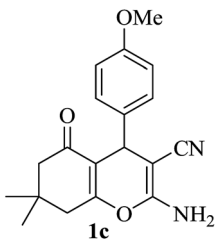 **1c**	10	93
04	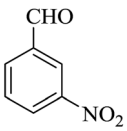	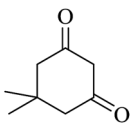	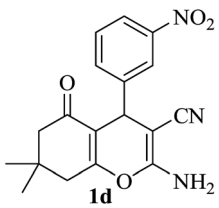 **1d**	15	91
05	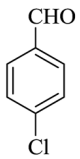	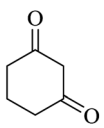	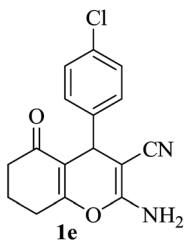 **1e**	10	92

Table 2 (*Contd.*)

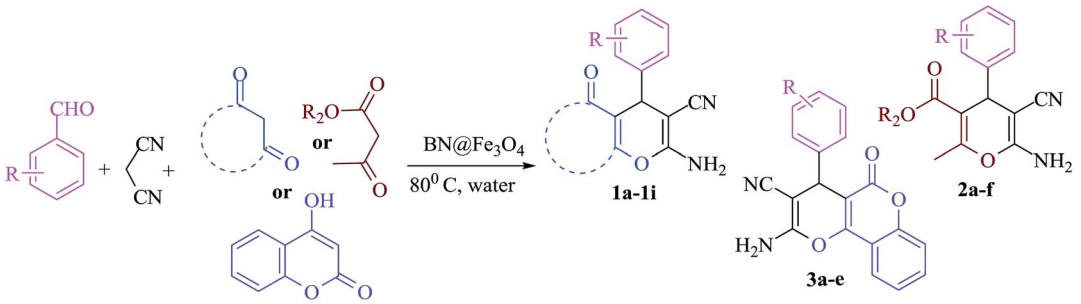

Run	Aldehyde	Diketones/4-hydroxy coumarine	Product	Time (min)	Yield[b] (%)
06	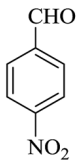	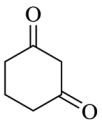	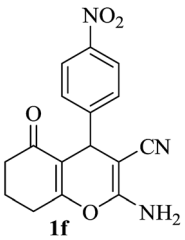 **1f**	15	90
07	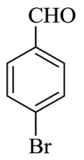	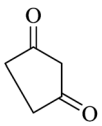	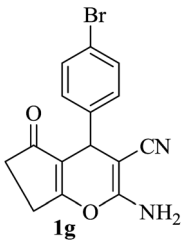 **1g**	15	89
08	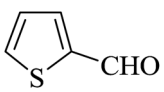	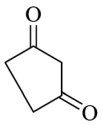	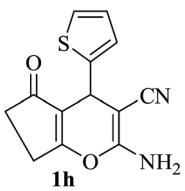 **1h**	20	86
09	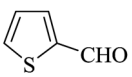	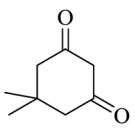	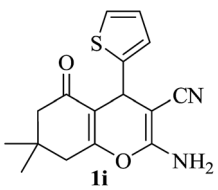 **1i**	15	88
10	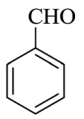	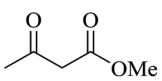	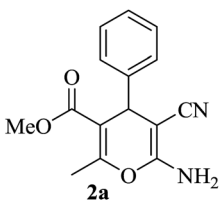 **2a**	15	95 91[c]
11	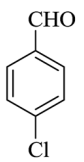	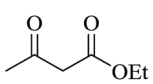	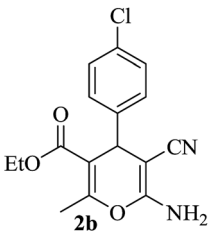 **2b**	15	94

Table 2 (*Contd.*)

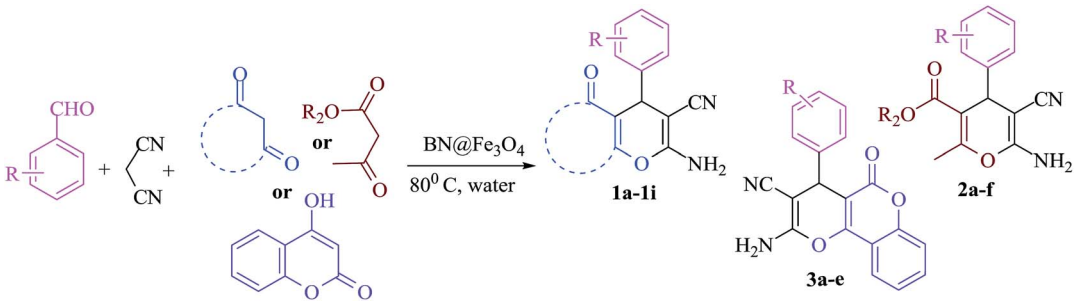

Run	Aldehyde	Diketones/4-hydroxy coumarine	Product	Time (min)	Yield[b] (%)
12	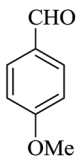	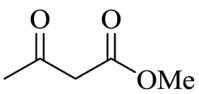	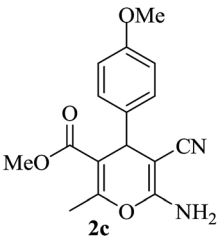 **2c**	15	93
13	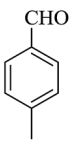	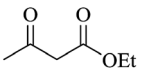	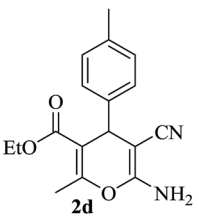 **2d**	15	94
14	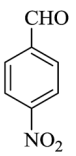	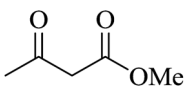	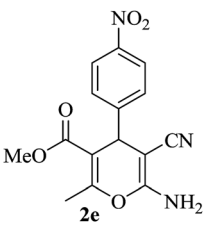 **2e**	20	92
15	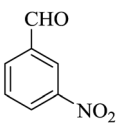	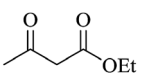	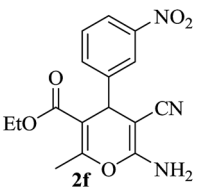 **2f**	20	90
16	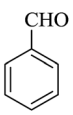	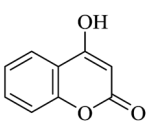	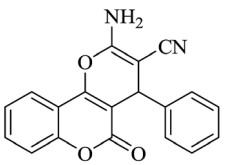 **3a**	20	95 90[c]
17	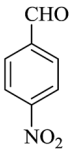	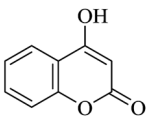	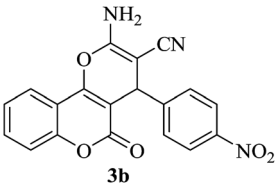 **3b**	25	90

Table 2 (*Contd.*)

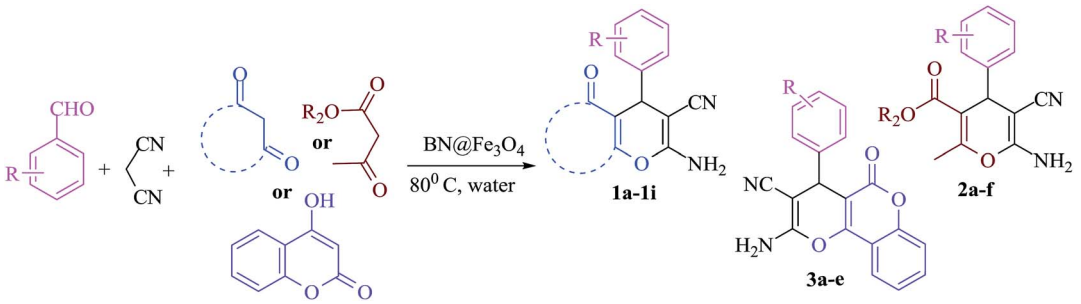

Run	Aldehyde	Diketones/4-hydroxy coumarine	Product	Time (min)	Yield[b] (%)
18	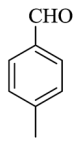	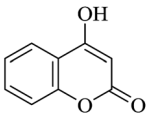	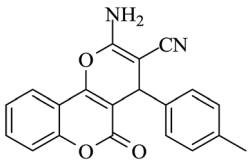 **3c**	20	92
19	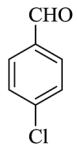	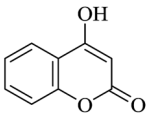	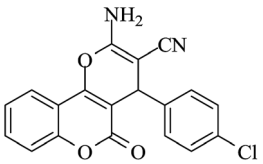 **3d**	10	94

[a] Reaction conditions: aldehyde (1.0 mmol), malononitrile (1.1 mmol) and cyclic diketones/1,3-diketoesters (1.0 mmol) or 4-hydroxycoumarine in 3 ml water at 80 °C. [b] Isolated yield. [c] Yield after 5th cycle.

solvent and temperature are summarized in Table 1. It was observed that trace amount of product was obtained in 3 hours without any catalyst in water at room temperature (Table 1, run 1). We initially tried reaction with 1 mg of catalyst ($BN@Fe_3O_4$) under the same condition as above and 15% of the product was obtained in 3 hours (Table 1, run 2). Increase in yield of the product was observed when the catalyst loading was increased to 5 mg or 10 mg using water (Table 1, run 3–4) or EtOH (Table 1, run 5) as solvent. When the reaction was carried out with 15 mg of catalyst at 60 °C, 80% of product (Table 1, run 7) was obtained whereas at room temperature only 60% of product (Table 1, run 6) was observed. On increasing the temperature of reaction to 80 °C, the reaction yield increases to 97% (Table 1, run 8). 94% of product was obtained (Table 1, run 9) with 15 mg of catalyst in EtOH under reflux condition. When the reaction was performed with 15 mg BN at room temperature and 80 °C, 52% and 68% product were obtained respectively (Table 1, run 10–11). Fe_3O_4 nanoparticles produced 65% of the product (Table 1, 12). We further increase the catalyst loading to 20 mg to check efficacy (Table 1, run 13) but the best result was obtained with 15 mg of catalyst on water at 80 °C. Accordingly, all the reactions discussed herein were conducted with this combination unless stated otherwise.

The reaction of various aromatic aldehydes having substituent such as Br, OMe and NO_2 were examined with malononitrile and dimedone under the optimized reaction conditions and the results are presented in Table 2 (run 1–4). In addition, the reaction of 1,3-cyclohexanedione or 1,3-cyclopentanedione was also carried out under similar reaction conditions with substituted aldehyde and malononitrile and 89–92% yield was obtained (Table 2, run 5–7). The heterocyclic aryl aldehyde also produced the corresponding product in good yields with same alacrity (Table 2, run 8 and 9). The scope of this methodology was also investigated with 1,3-diketoesters using aldehyde and malononitrile. It is important to note that the reaction occurred at room temperature in 15 minutes. It is evident from Table 2 that nitro substituted aldehyde took little longer reaction time and give comparatively lower yield (run 14 and 15).

To demonstrate the scope, the reactions of various aromatic aldehydes were examined with malononitrile and 4-hydroxycoumarin under identical reaction conditions and the results are in Table 2 (run 16–19). Heterocyclic aldehyde also furnish product in good yield (Table 2, run 20).

Under similar experimental conditions, we further use isatin or substituted isatin (Cl and Br) instead of aldehyde with malononitrile and dimedone or cyclohexane-1,3-dione or cyclopentane-1,3-dione to check the efficacy of catalyst. The reaction proceeds well and the products were isolated in good yields (Table 3). The scope of this procedure was further extended

Table 3 $BN@Fe_3O_4$ catalyzed synthesis of highly functionalized spirooxindole with isatin, malononitrile and cycloalkane-1,3-dione (**4a–e**)[a] or 1,3-diketoesters (**5a–d**)[a]

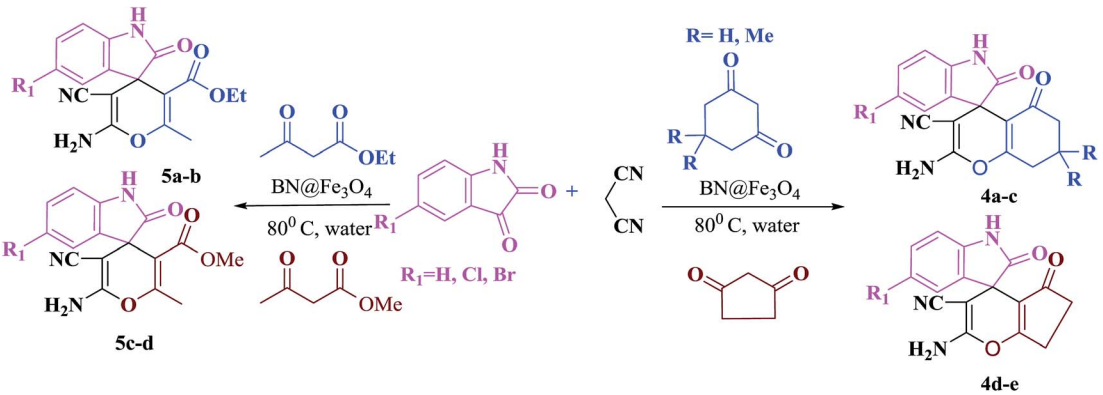

Run	Isatin	Active methylene	Diketones	Product	Time (min)	Yield[b] (%)
01	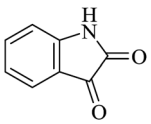		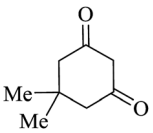	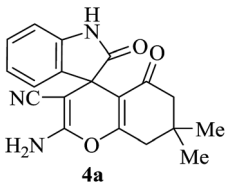 **4a**	30	92 88[c]
02	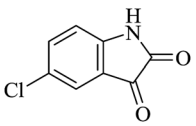		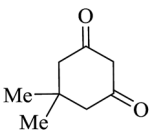	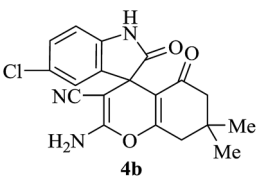 **4b**	30	91
03	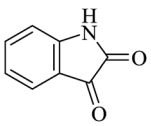		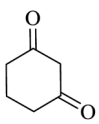	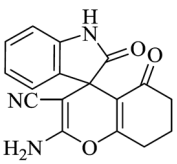 **4c**	30	90
04	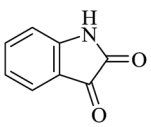		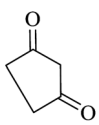	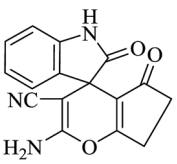 **4d**	45	88
05	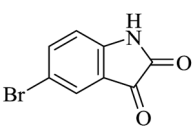		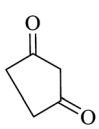	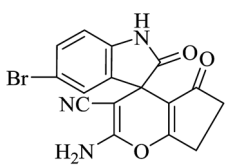 **4e**	45	87
06	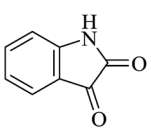		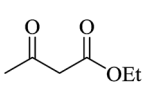	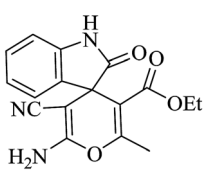 **5a**	60	93 89[c]

Table 3 (*Contd.*)

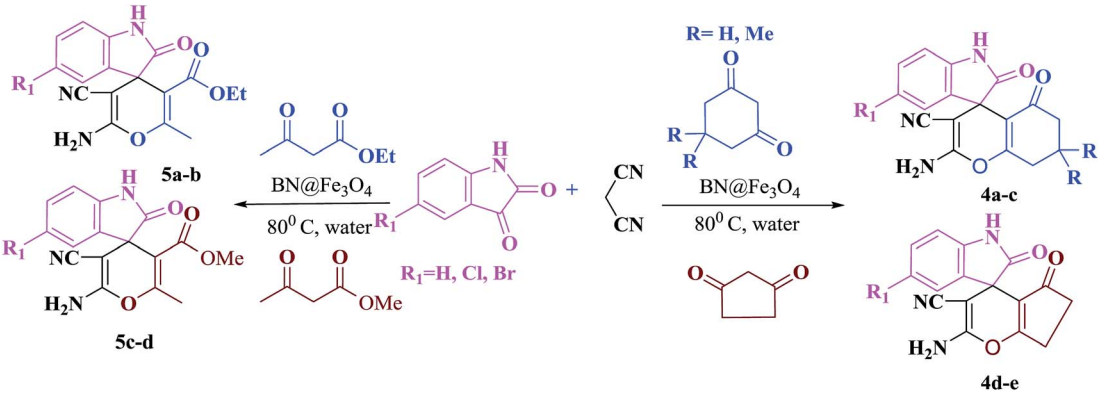

Run	Isatin	Active methylene	Diketones	Product	Time (min)	Yield[b] (%)
07	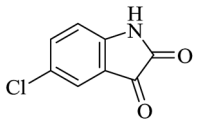		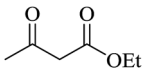	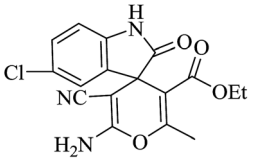 **5b**	60	88
08	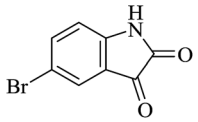		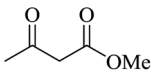	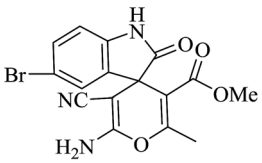 **5c**	60	90
09	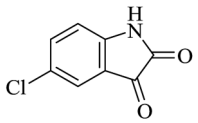		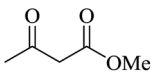	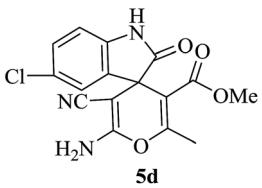 **5d**	60	89

[a] Reaction conditions: isatin derivatives (1.0 mmol), malononitrile (1.1 mmol) and cyclic-1,3-diketone or 1,3-diketoesters (1.0 mmol) in 3 ml water under 80 °C. [b] Isolated yield. [c] Yield after 5th cycle.

to 1,3-diketoesters using isatin and malononitrile. The reactions get completed in one hour with 89–93% yield (Table 3, run 6–9).

In order to expand the panorama of this methodology, we carried out reactions of 4-hydroxy-coumarin with isatin and malononitrile and the results are summarized in Table 4 (run 1–2). Reaction of 4-hydroxy-6-methyl-2*H*-pyran-2-one with isatin and malononitrile take little longer time to furnish the desired product (Table 4, run 3). Under the similar reaction condition, barbituric acid or 2-thiobarbituric acid also furnished the desired spirooxindole derivatives with same rapidity (Table 4, run 4–7).

A mechanistic pathway is proposed for the formation of highly functionalised spirooxindole derivatives in Scheme 2. According to our planned methodology, this domino reaction proceeds through Knoevenagel condensation followed by Michael addition. Knoevenagel condensation occurs at faster rate with activation of carbonyl group by the "Boron" end of the nanocomposites, while basic nature of iron oxide helps to abstract proton from malononitrile and 1,3 diketo compounds. It is also established from our previous work[9] that BN efficiently catalyses Michael addition. Initially, isatin reacts with malononitrile to give Knoevenagel condensation product (**1**). 1,3-Diketone and electron deficient Knoevenagel condensation product (**1**) undergo Michael addition to give the intermediate product (**2**). Enolization of the intermediate (**2**) occurs followed by intramolecular cyclization and rearrangement through **3** and **4** to give the corresponding spirooxindole derivatives **5**. To the end, catalyst reusability (Fig. 4) was performed for the synthesis of different substrate, **1a**, **2a**, **3a**, **4a**, **5a** and **6a**. The catalyst showed nearly consistent activity for at least five reaction cycles (Table 2, run 1, 10 and 16; Table 3, run 1 and 6; Table 4, run 1). The comparison of reported methods and the present results

Table 4 $BN@Fe_3O_4$ catalyzed synthesis of highly functionalized spirooxindole with isatin, malononitrile and 4-hydroxy-derivatives or barbituric acid or 2-thiobarbituric (**6a–g**)[a]

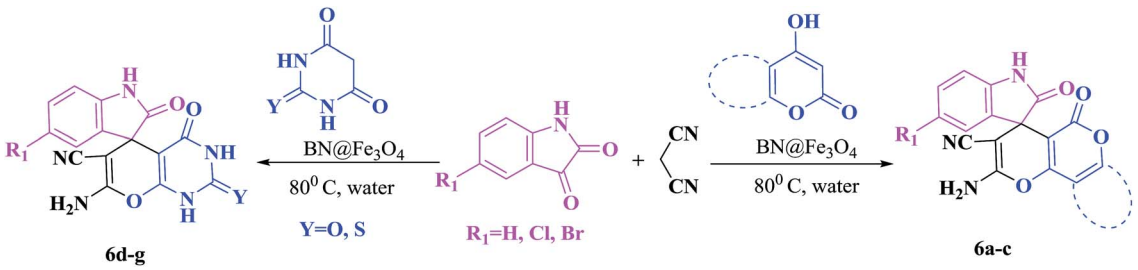

Run	Isatin	4-Hydroxy derivatives or barbituric/thiobarbituric acid	Product	Time (min)	Yield[b] (%)
01	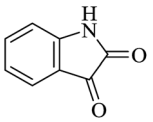	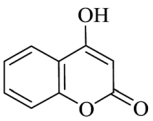	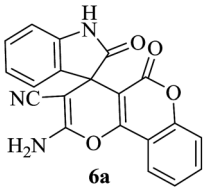 **6a**	45	88 84[c]
02	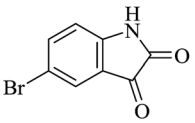	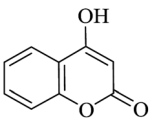	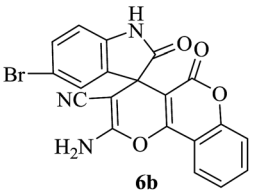 **6b**	45	86
03	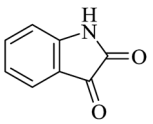	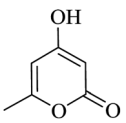	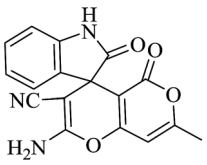 **6c**	60	85
04	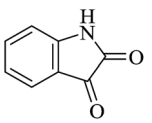	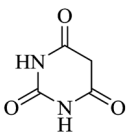	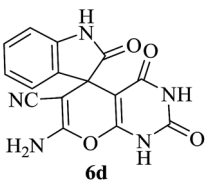 **6d**	45	88
05	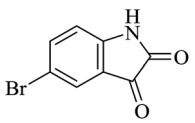	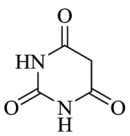	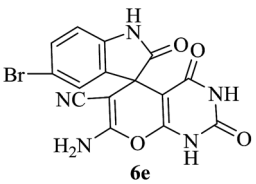 **6e**	45	86
06	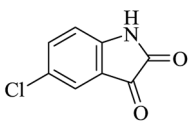	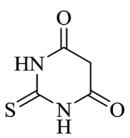	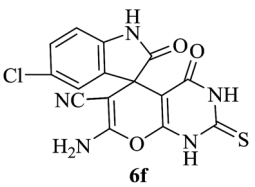 **6f**	60	90
07	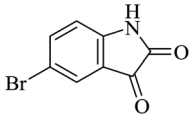	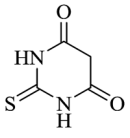	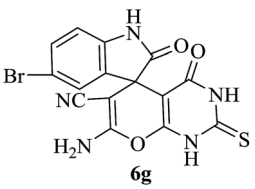 **6g**	60	90

Table 4 (*Contd.*)

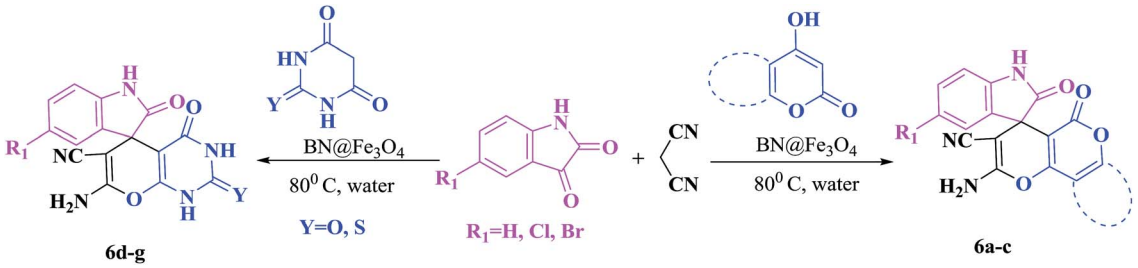

Run	Isatin	4-Hydroxy derivatives or barbituric/thiobarbituric acid	Product	Time (min)	Yield[b] (%)

[a] Reaction conditions: isatin derivatives (1.0 mmol), malononitrile (1.1 mmol) and 4-hydroxy derivatives or barbituric acid/thiobarbituric acid (1.0 mmol) in 3 ml water under 80 °C. [b] Isolated yield. [c] Yield after 5th cycle.

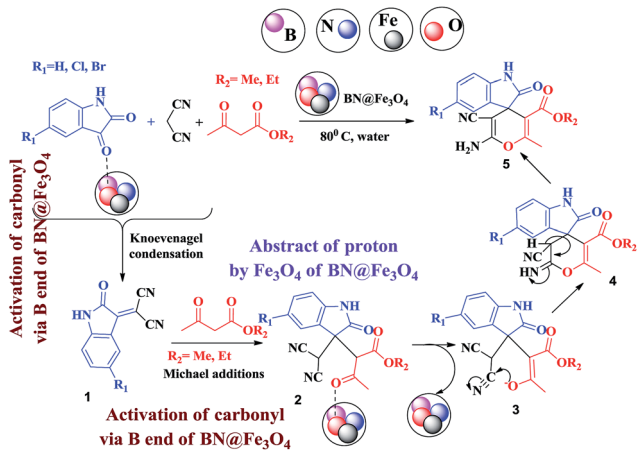

Scheme 2 Proposed mechanism for the synthesis of highly functionalised spirooxindole derivatives.

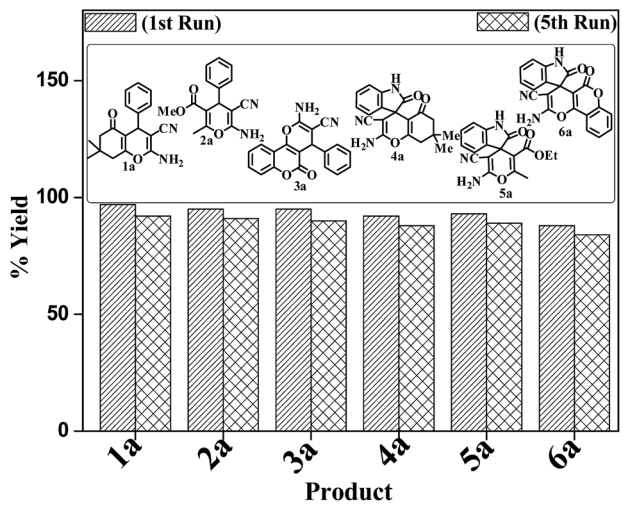

Fig. 4 Reusability of $BN@Fe_3O_4$ with different substrates 1a, 2a, 3a, 4a, 5a and 6a.

Table 5 Comparison of synthesis of pyran derivatives with reported protocols for compound 1a

Sl no.	Catalyst (ref. 33)	Reaction conditions (temp./solvent/time)	Yield
1	$Ni(NO_3)_2 \cdot 6H_2O$	Refluxing/H_2O/20 min	88
2	Pd nanoparticles	Refluxing/CH_3CN/4.2 h	88
3	PPA-SiO_2	Refluxing/H_2O/10 min	93
4	Amberlyst A21	RT/EtOH/1 h	84
5	SB-DABCO	RT/EtOH/25 min	95
6	DMAP	Refluxing/EtOH/15 min	94
7	MgO	RT/neat/25 min	86
8	*N*-Methylimidazole	RT/H_2O/90 min	90
9	$BN@Fe_3O_4$	Refluxing/H_2O/10 min	97

are charted in Table 5. It is clear from the table that the present protocol is better than the reported protocols with respect to time, solvent and yields.

In conclusion, a new catalyst $BN@Fe_3O_4$ has been developed and characterized by powder XRD, FT-IR, Raman, BET and FE-SEM. It efficiently catalyzes the formation of highly functionalized pyrans and spirooxindoles derivatives of potential synthetic and pharmacological interest in domino fashion. This protocol offers diverse advantages such as the high yields of product without any column chromatography, simple work-up and use of inexpensive and recyclable catalyst. It is also capable of working efficiently on water thereby satisfying some principle of "Green Chemistry".

Acknowledgements

A. M is thankful to IIT Patna for his research fellowship. Authors are thankful to SAIF (Panjab University, Chandigarh) and IIT Kanpur and IISER Kolkata for NMR facility.

References

1 A. Corma, H. Garcia and F. X. Llabrés i Xamena, *Chem. Rev.*, 2010, **110**, 4606–4655.

2 M. B. Gawande, P. S. Branco and R. S. Varma, *Chem. Soc. Rev.*, 2013, **42**, 3371–3393.
3 C. N. R. Rao, A. Müller and A. K. Cheetham, *The Chemistry of nanomaterials*, Wiley-VCH Verlag GmbH & Co. KGaA, 2005, pp. 1–11.
4 G. Schmid, *Chem. Rev.*, 1992, **92**, 1709–1727.
5 N. T. S. Phan, C. S. Gill, J. V. Nguyen, Z. J. Zhang and C. W. Jones, *Angew. Chem., Int. Ed.*, 2006, **45**, 2209–2212.
6 I. Bauer and H.-J. Knölker, *Chem. Rev.*, 2015, **115**, 3170–3387.
7 A. Primo, S. Navalón, A. M. Asiri and H. García, *Chem.–Eur. J.*, 2015, **21**, 324–330.
8 L. Wang, C. Sun, L. Xu and Y. Qian, *Catal. Sci. Technol.*, 2011, **1**, 1119–1123.
9 A. Molla and S. Hussain, *Curr. Catal.*, 2013, **2**, 88–95.
10 A. Nag, K. Raidongia, K. P. S. S. Hembram, R. Datta, U. V. Waghmare and C. N. R. Rao, *ACS Nano*, 2010, **4**, 1539–1544.
11 S. Rostamizadeh, N. Shadjou, M. Azad and N. Jalali, *Catal. Commun.*, 2012, **26**, 218–224.
12 D. Wang and D. Astruc, *Chem. Rev.*, 2014, **114**, 6949–6985.
13 R. B. N. Baig, M. N. Nadagouda and R. S. Varma, *Coord. Chem. Rev.*, 2015, **287**, 137–156.
14 R. Hudson, Y. Feng, R. S. Varma and A. Moores, *Green Chem.*, 2014, **16**, 4493–4505.
15 V. Polshettiwar, R. Luque, A. Fihri, H. Zhu, M. Bouhrara and J.-M. Basset, *Chem. Rev.*, 2011, **111**, 3036–3075.
16 J. Hua and Y. HeQing, *Sci. China, Ser. E: Technol. Sci.*, 2008, **51**, 1911–1920.
17 N. Islam, L. V. Phong, J. R. Jeong and C. G. Kim, *Thin Solid Films*, 2011, **519**, 8277–8279.
18 Y. Deng, L. Wang, W. Yang and S. Fu, *J. Magn. Magn. Mater.*, 2003, **257**, 69–78.
19 S. Franger, P. Berthet and J. Berthon, *J. Solid State Electrochem.*, 2004, **8**, 218–223.
20 W. Wu, Q. He and C. Jiang, *Nanoscale Res. Lett.*, 2008, **3**, 397–415.
21 R. Y. Honga, T. T. Pan and H. Z. Li, *J. Magn. Magn. Mater.*, 2006, **303**, 60–68.
22 H. Hu, H. Yang, P. Huang, D. Cui, Y. Peng, J. Zhang, F. Lu, J. Lian and D. Shi, *Chem. Commun.*, 2010, **46**, 3866–3868.
23 C. Li, Y. Wei, A. Liivat, Y. Zhu and J. Zhu, *Mater. Lett.*, 2013, **107**, 23–26.
24 L. F. Tietze, G. Brasche and K. Gericke, *Domino reactions in organic synthesis*, Wiley-VCH, Weinheim, 1996.
25 B. Ganem, *Acc. Chem. Res.*, 2009, **42**, 463–472.
26 M. M. C. Lo, C. S. Newmann, S. Nagayams, E. O. Perlstein and S. L. Schreiber, *J. Am. Chem. Soc.*, 2005, **127**, 10130–10131.
27 M. M. G. Kumari, *Eur. J. Med. Chem.*, 2011, **46**, 1181–1188.
28 B. K. S. Yeung, B. Zou, M. Rottmann, S. B. Lakshminarayana, S. H. Ang, S. Y. Leong, J. Tan, J. Wong, S. Keller-Maerki, C. Fischli, A. Goh, E. K. Schmitt, P. Krastel, E. Francotte, K. Kuhen, D. Plouffe, K. Henson, T. Wagner, E. A. Winzeler, F. Petersen, R. Brun, V. Dartois, T. T. Diagana and T. H. Keller, *J. Med. Chem.*, 2010, **53**, 5155–5164.
29 V. V. Vintonyak, K. Warburg, H. Kruse, S. Grimme, K. Hübel, D. Rauh and H. Waldmann, *Angew. Chem., Int. Ed.*, 2010, **49**, 5902–5905.
30 P. K. Paliwal, S. R. Jetti and S. Jain, *Med. Chem. Res.*, 2013, **22**, 2984–2990.
31 A.-G. E. Amr, A. M. Mohamed, S. F. Mohamed, N. A. Abdel-Hafez and A. E.-F. G. Hammam, *Bioorg. Med. Chem.*, 2006, **14**, 5481–5488.
32 D. Kumar, V. B. Reddy, S. Sharad, U. Dube and S. A. Kapur, *Eur. J. Med. Chem.*, 2009, **44**, 3805–3809.
33 (*a*) B. Boumoud, A. A. Yahiaoui, T. Boumoud and A. Debache, *J. Chem. Pharm. Res.*, 2012, **4**, 795–799; (*b*) M. Saha and A. K. Pal, *Adv. Nanopart.*, 2012, **1**, 61–70; (*c*) A. Davoodnia, S. Allameh, S. Fazli and N. T. Hoseini, *Chem. Pap.*, 2011, **65**, 714–720; (*d*) M. Bihani, P. P. Bora, G. Bez and H. Askari, *C. R. Chim.*, 2013, **16**, 419–426; (*e*) A. Hasaninejad, M. Shekouhy, N. Golzar, A. Zare and M. M. Doroodmand, *Appl. Catal., A*, 2011, **402**, 11–22; (*f*) A. T. Khan, M. Lal, S. Ali and M. M. Khan, *Tetrahedron Lett.*, 2011, **52**, 5327–5332; (*g*) D. Kumar, V. B. Reddy, S. Sharad, U. Dube and S. Kapur, *Eur. J. Med. Chem.*, 2009, **44**, 3805–3809; (*h*) X. Z. Lian, Y. Huang, Y. Q. Li and W. J. Zheng, *Monatsh. Chem.*, 2008, **139**, 129–131.
34 (*a*) H. Hagiwara, A. Numamae, K. Isobe, T. Hoshi and T. Suzuki, *Heterocycles*, 2006, **68**, 889–895; (*b*) S. B. Bandgar, B. P. Bandgar, B. L. Korbad, J. V. Totre and S. Patil, *Aust. J. Chem.*, 2007, **60**, 305–307; (*c*) M. A. Zolfigol, A. Khazaei, A. R. Moosavi-Zare, J. Afsar, V. Khakyzadeh and O. Khaledian, *J. Chin. Chem. Soc.*, 2015, **62**, 398–403; (*d*) G. M. Ziarani, A. Badiei, S. Mousavi, N. Lashgari and A. Shahbazi, *Chin. J. Catal.*, 2012, **33**, 1832–1839; (*e*) M. Hosseini-Sarvari and M. Tavakolian, *Comb. Chem. High Throughput Screening*, 2012, **15**, 826–834; (*f*) M. A. Nasseri, F. Kamali and B. Zakerinasab, *RSC Adv.*, 2015, **5**, 26517–26520; (*g*) N. Lashgari, G. M. Ziarani, A. Badiei and M. Zarezadeh-Mehrizib, *J. Heterocycl. Chem.*, 2014, **51**, 1628–1633; (*h*) H. R. Safaei, M. Shekouhy, S. Rahmanpur and A. Shirinfeshan, *Green Chem.*, 2012, **14**, 1696–1704; (*i*) R. Y. Guo, Z. M. An, L. P. Mo, R. Z. Wang, H. X. Liu, S. X. Wang and Z. H. Zhang, *ACS Comb. Sci.*, 2013, **15**, 557–563; (*j*) A. Khalafi-Nezhad, E. S. Shahidzadeh, S. Sarikhani and F. Panahi, *J. Mol. Catal. A: Chem.*, 2013, **379**, 1–8; (*k*) R. Sridhar, B. Srinivas, B. Madhav, V. P. Reddy, Y. V. D. Nageswar and K. R. Rao, *Can. J. Chem.*, 2009, **87**, 1704–1707; (*l*) G. M. Ziarani, S. Faramarzi, N. Lashgari and A. Badiei, *J. Iran. Chem. Soc.*, 2014, **11**, 701–709; (*m*) A. Rostami, B. Atashkar and H. Gholami, *Catal. Commun.*, 2013, **37**, 69–74; (*n*) A. Saha, S. Payra and S. Banerjee, *RSC Adv.*, 2015, **5**, 101664–101671; (*o*) Y. Li, H. Chen, C. Shi, D. Shi and S. Ji, *J. Comb. Chem.*, 2010, **12**, 231–237.
35 C. Y. Zhi, Y. Bando, C. C. Tang and D. Golberg, *Appl. Phys. Lett.*, 2005, **86**, 213110–213113.
36 R. Geick, C. H. Perry and G. Rupprecht, *Phys. Rev.*, 1966, **146**, 543–547.
37 S. Reich, A. C. Ferrari, R. Arenal, A. Loiseau, I. Bello and J. R. Roberton, *Phys. Rev. B: Condens. Matter Mater. Phys.*, 2005, **71**, 205201–205212.

